ENDOCARDIAL MOTION ESTIMATION FROM ELECTRO-ANATOMICAL DATA

A. R. Porras ⋆*, G. Piella* ⋆*, C. Hoogendoorn* ⋆*, D. Andreu* †*, A. Berruezo* †*, A. F. Frangi* ⋆‡

⋆ CISTIB - Universitat Pompeu Fabra, CIBER-BBN, Barcelona, Spain.
† Hospital Clinic, IDIBAPS, Universitat de Barcelona, Barcelona, Spain.
‡ Department of Mechanical Engineering, University of Sheffield, Sheffield, UK.

ABSTRACT

An accurate scar characterization plays an essential role for the treatment of ventricular tachycardia in patients with ischemic cardiomyopathy. Cardiac ablation based on electrical information is a widely used procedure to fix ventricular tachycardia. However, intra-operative scar characterization may be improved using mechanical information together with the electrical data. We propose in this paper a method to reconstruct the endocardial motion intra-operatively by exploiting both information from an electro-anatomical mapping system and the heart anatomy segmented from any pre-operative 3D imaging modality, using a bilinear statistical atlas to approximate motion in the areas where no information is provided. We applied the proposed methodology to four patients with ischemic cardiomyopathy. The results showed abnormal strain curves in presence of scar, which was defined using contrast-enhanced magnetic resonance images.

1. INTRODUCTION

Ischemic cardiomyopathy (IC) is a coronary artery disease that causes lack of oxygen supply to some parts of the myocardial tissue. Consequently, myocardial cells die and some areas of dense fibrosis appear where electrical impulse cannot be propagated. Close to these areas, it is often possible to find areas with low density fibrosis that still have electrical activity, even though conduction is slow. Sometimes, these areas describe paths through or around fibrotic tissue creating a re-entrance mechanism that produces an asynchronous ventricle contraction called ventricular tachycardia (VT) [1].

When VT cannot be successfully controlled with anti-arrhythmic drugs, catheter ablation has been demonstrated to be a good option to treat the tachycardia. Therefore, intra-operative scar characterization is a key factor for an effective treatment. Nowadays, this characterization is done based only on the electrical signals recorded with the catheter tip. However, it presents some problems, such as far field effect, bad signal/noise ratio and the lack of a standard threshold valid for all patients [2]. Hence, it would be desirable to have more information on the ventricle's behavior to make decisions intra-operatively, as it is the case of motion and strain information. A new method to obtain the ventricle's endocardial motion and strain is presented in this paper, and the obtained information is analyzed together with the electrical data.

Some studies have been carried out to extract motion information intra-operatively from electro-anatomic mapping (EAM) data. In [3], a novel technique to combine electrical activation and motion information from an EAM was presented as part of the NOGA system (Biologics Delivery Systems Group, Cordis Corporation, Irwindale CA, USA). In [4], a methodology to obtain endocardial motion from EAM systems was proposed, and the possibility of identifying motion patterns to predict septal flash was shown. In [5], an endocardial end-systolic deformation was calculated and a correlation between low strain values and low bipolar voltages was found. However, according to our knowledge, this is the first work where a reconstruction of the whole endocardial motion from EAM data is performed.

2. METHODOLOGY

For the present study, maps from four patients with ischemic cardiomyopathy were used, acquired with Carto system (Biosense Webster, Haifa, Israel). The maps contain both electrical signals acquired with the catheter tip and its position information sampled at 1 KHz and 100 Hz respectively, with an average of 441.75 ± 106.27 points.

2.1. Position signals filtering and re-synchronization

With an EAM system, a set of points with electrical and position information is created, being each point acquired independently from the others. Catheter position signals obtained can be considered as the addition of four main signals of different nature: ventricle motion, respiratory motion, catheter sliding over the wall, and random noise associated to the tracking system.

We are interested in ventricular motion, so it is necessary to filter out the other three components. Since resting heart

This research has been partially funded by the Industrial and Technological Development Center (CDTI) under the CENIT-cvREMOD program. A. F. Frangi is partially funded by the ICREA-Academia program.

rate is about 60-100 bpm for an adult and the mean respiration rate at rest is about 12-20 bpm [6], it is possible to minimize the respiration effect by applying a high-pass frequency filter. In addition, a low-pass filter can also be used to filter out the high frequency noise present because of the tracking error of the system. Therefore, we propose a Butterworth band-pass filter with cutoff frequencies of 0.7 and 10 Hz, thus assuming a heart rate greater than 42 bpm.

Catheter movement with respect to the ventricular wall presents unreliable local motion patterns. Points with a drift of 5 mm between consecutive end-diastolic positions were considered unreliable and, therefore, discarded.

Finally, since motion information is not synchronized among different points, all motion signals are processed so that one beat is extracted and resampled to a fixed duration. We chose a length of 200 samples, thus avoiding the loss of position information.

2.2. Points-to-shape registration

To identify the correspondence of every acquired point to its spatial location in the ventricle, the set of points is registered to a mesh obtained pre-operatively by segmenting it from any 3D imaging modality. We used magnetic resonance imaging (MRI) data for this work.

For registration, three landmarks were placed both in the cloud of points from the mapping system and the segmented mesh (two in the aorta and one in the apex). Then, after a landmark-based rigid registration, an Iterative Closest Point (ICP) algorithm is used to better adjust the points to the mesh.

2.3. Endocardial motion estimation

The main idea to recover endocardial motion is to deform the endocardial shape (segmented from any pre-operative imaging modality) using the motion signals obtained intra-operatively from the EAM system. However, the spatial resolution of the electro-anatomic map is very low and the points are usually concentrated at the area of interest for the electrophysiologist, so this map cannot be used directly to obtain a reliable motion reconstruction.

For those reasons, we propose the use of a statistical atlas that allows estimating motion in the areas where no motion information is provided by the EAM system. Since we have two different types of information (end-diastolic endocardial shape obtained pre-operatively and the sparse motion information acquired intra-operatively), a bilinear atlas that separately codes shape and motion was used.

We used a bilinear atlas built from 80 patients and 15 phases in the cardiac cycle, constructed from segmented meshes of 880 points as described in [7]. According to this, the endocardial shape for a subject *s* at a time instant *i* can be estimated as:

$$\mathbf{y_i^s} = (\mathbf{W b_i})^{\mathbf{VT}} \mathbf{a^s} \tag{1}$$

where $\mathbf{y_i^s}$ represents the shape of the subject *s* in the phase *i* of the cardiac cycle, $\mathbf{a^s}$ is a parameters vector representing the subject *s*, $\mathbf{b_i}$ is a parameters vector representing the phase *i* of the cardiac cycle, $\mathbf{W}$ is a constant matrix governing the interaction between the factors and VT is the vector transpose operation as explained in [7].

Since we know the endocardial shape in end diastole, we can use (1) to solve for $\mathbf{a^s}$, using the $\mathbf{b_i}$ vector associated to end diastole in the atlas:

$$\mathbf{a^s} = \left((\mathbf{W b_i})^{\mathbf{VT}}\right)^{-1} \mathbf{y_i^s}. \tag{2}$$

To solve for the $\mathbf{b_i}$ vectors describing each phase of the cardiac cycle, we can propagate the motion information recorded for each point by the EAM system into its correspondence in the pre-operative shape. Thus, we can solve (3) using only the points from which we have motion information, using the $\mathbf{a^s}$ calculated in (2):

$$\mathbf{b_i} = \left((\mathbf{W^{VT} a^s})^{\mathbf{VT}}\right)^{-1} \mathbf{y_i^s}. \tag{3}$$

2.4. Endocardial strain estimation

Let $\mathbf{u}$ be the displacement vector of a point at certain phase of the cardiac cycle, obtained by subtracting the position of the point in end diastole to the one in the current phase. Then, the strain tensor ϵ can be calculated with the following equation:

$$\epsilon = \frac{\mathbf{1}}{\mathbf{2}}(\bigtriangledown \mathbf{u^T} + \bigtriangledown \mathbf{u} + \bigtriangledown \mathbf{u} \bigtriangledown \mathbf{u^T}) \tag{4}$$

where $\bigtriangledown \mathbf{u}$ denotes the spatial derivatives of the displacement vector, calculated at the center of every triangle of the mesh using linear shape functions. The strain tensor is projected in both longitudinal and circumferential directions to obtain directional strains. Radial strain cannot be reliably estimated because there is no information about wall thickening.

3. EXPERIMENTS AND RESULTS

Strain was calculated as previously explained and was related to the recorded electrical activity. We performed the experiments on four patients, finding abnormal strain curves where scar tissue was present. These abnormalities were more evident on the circumferential component of the strain tensor.

We sought to study the spatio-temporal relation between mechanical and electrical events by comparing maximum voltages (both bipolar and unipolar), local activation times, motion and strain information in presence of scar. To present our findings graphically, we show detailed results for one subject, with scar in AHA segments 3 through 6, 10 and 11 (see Fig. 1a), with transmurality and density greatest in segment 5. For the remaining three subjects we present circumferential strain curves.

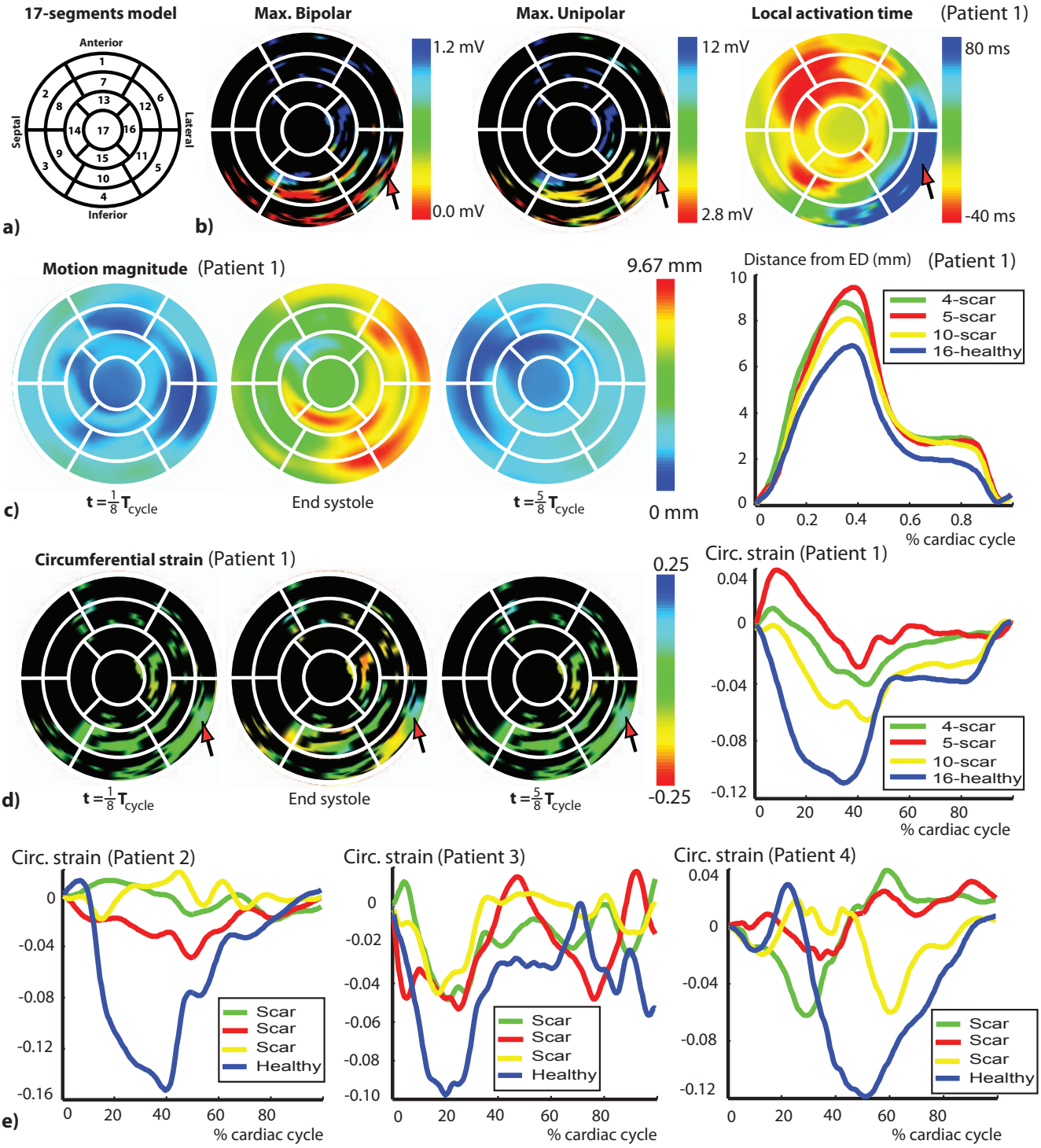


Fig. 1. **(a)** shows the American Heart Association (AHA) "bulls-eye" plot template. (**b**), (**c**) and (**d**) show the results for the same patient. (**b**) shows the electrical information obtained from the EAM system. Maximum bipolar and unipolar voltages are color-coded; black indicates no information, arrow indicates highest scar density. Local activation time was calculated from the electro-anatomical data and interpolated for the whole endocardium. Motion magnitude (**c**) and circumferential strain (**d**) are shown on bulls-eye for three time points in the cardiac cycle, and over the full cycle for four segments. (**e**) shows the circumferential strain curves computed for three scarred and one healthy segment for the remaining three subjects.

Fig.1.b shows the maximum bipolar and unipolar voltages for the areas where we have information from the EAM system, together with the local activation time (which is the delay of the maximum bipolar peak with respect to the R-peak of the ECG) interpolated over the endocardial shape. As can be observed, both unipolar and bipolar voltages are low in the areas affected by the scar, being the unipolar voltage even lower where the transmurality of the scar is higher. The local activation time shows an activation delay in the scar that is even longer in the segment with the highest scar transmurality.

Fig.1.c shows the motion magnitude at three different phases of the cardiac cycle and its evolution during the cardiac cycle in four different segments of the endocardium. Both the magnitude and shape of motion curves are very similar between scarred and healthy segments. One explanation for that is that non-deforming regions can show passive motion due to tethering to adjacent regions and overall heart motion [8]. Moreover, it is possible to appreciate that motion magnitude is low in comparison to [9], probably because of the presence of the scar.

Fig.1.d shows the circumferential strain calculated only for the areas where we have electro-anatomical information, because it is a differential measure and any estimation in other areas would be unreliable. The evolution of the circumferential strain at four different segments of the endocardium is also shown in Fig.1.d. AHA segment 16, which corresponds to a healthy area of the endocardium, shows a contraction from end diastole to end systole, returning later to its initial state at the next end diastole. However, the curves of strain calculated for the other segments do not present the same shape. We can appreciate an initial stretching, which is more pronounced in the area where the scar transmurality is higher (segment 5). In addition, the duration of this stretching interval is higher in segment 5, which could be related to a longer delay in the electrical activation. We want to stress that the strain magnitude calculated for all the segments is low compared to normal subjects [10]. This was expected because the scar might affect the global contraction of the myocardial wall, and not only the area where it is present.

Finally, Fig.1.e also shows the circumferential strain curves for three other patients, obtaining results similar to those for the first subject.

These results suggest that strain calculated intra-operatively with the proposed method could help to identify the areas where scar is present.

4. CONCLUSIONS

A novel method to recover the motion of the LV endocardium intra-operatively from EAM data was presented. Relationships between strain, local activation time and maximum voltages have been found, being the strain related to the density and transmurality of the scar, and the contraction delay related to the local activation time. The results are encouraging enough to test this on a larger population.

To improve our methodology, an atlas built from more patients could be used to include more variability in ventricular motion.

5. REFERENCES

[1] W. G. Stevenson, "Ventricular scars and ventricular tachycardia," *Trans. Am. Clin. Climat. Assoc.*, vol. 120, pp. 403–412, 2009.

[2] H. E. Botker, J. F. Lassen, F. Hermansen, H. Wiggers, P. Sogaard, W. Y. Kim, M. Bottcher, L. Thuesen, and A. K. Pedersen, "Electromechanical mapping for detection of myocardial viability in patients with ischemic cardiomyopathy," *Circulation*, vol. 103, pp. 1631–1637, 2001.

[3] H. U. Klemm, R. Ventura, O. Franzen, S. Baldus, K. Mortensen, T. Risius, and Willems S., "Simultaneous mapping of activation and motion timing in the healthy and chronically ischemic heart," *Heart Rhythm*, vol. 3, no. 7, pp. 781–788, 2006.

[4] O. Camara, S. Oeltze, M. De Craene, R. Sebastian, E. Silva, D. Tamborero, L. Mont, M. Sitges, B. J. Bijnens, and A. F. Frangi, "Cardiac motion estimation from intracardiac electrical mapping data: Identifying a septal flash in heart failure," in *FIMH*, vol. 5528 of *LNCS*, pp. 21–29. 2009.

[5] A. R. Porras, G. Piella, O. Camara, E. Silva, D. Andreu, A. Berruezo, and A. F. Frangi, "Cardiac deformation from electro-anatomical mapping data: Application to scar characterization," in *FIMH*, vol. 6666 of *LNSC*, pp. 47–54. Springer Berlin / Heidelberg, 2011.

[6] G. J. Tortora and N. P. Anagnostakos, *Principles of Anatomy and Physiology, 6th edition, New York: Harper-Collins, 1990, p. 707*, Harper-Collins, 6th edition edition, 1990.

[7] C. Hoogendoorn, F. M. Sukno, S. Ordas, and A. F. Frangi, "Bilinear models for spatio-temporal point distribution analysis: Application to extrapolation of whole heart cardiac dynamics," *Int. J. Computer Vision*, vol. 85(3), pp. 237–252, 2009.

[8] J. Gorcsan, "Echocardiographic strain imaging for myocardial viability: An improvement over visual assessment," *Circulation*, vol. 112, no. 25, pp. 3820–3822, 2005.

[9] P. Germain, G. Roul, A. Constantinesco, P. M. Coulbois, J. Baruthio, J. M. Mossard, P. Bareiss, and A. Sacrez, "Comparison between abnormalities in segmental endocardial motion and abnormalities in segmental wall thickening after anterior myocardial infarction," *Eur. Heart J.*, vol. 17, no. 9, pp. 1350–1361, 1996.

[10] C. C. Moore, C. H. Lugo-Olivieri, E. R. McVeigh, and E. A. Zerhouni, "Three-dimensional systolic strain patterns in the normal human left ventricle: characterization with tagged mr imaging.," *Radiology*, vol. 214, no. 2, pp. 453–466, 2000.